

# Short-term variability of photospheric lines in the pre-main sequence Herbig Ae star AB Aurigae<sup>\*</sup>

C. Catala<sup>1</sup>, T. Böhm<sup>2</sup>, J.-F. Donati<sup>1</sup>, T. Simon<sup>3</sup>, S. Jiang<sup>4</sup>, and F. Zhao<sup>4</sup>

<sup>1</sup> Laboratoire d'Astrophysique de Toulouse, CNRS URA 285, Observatoire Midi-Pyrénées, 14, avenue Edouard Belin, F-31400 Toulouse, France

<sup>2</sup> European Southern Observatory, Karl-Schwarzschildstrasse 2, D-85748 Garching bei München, Germany

<sup>3</sup> Institute for Astronomy, University of Hawaii, 2680 Woodlawn Drive, Honolulu, Hawaii 96822, USA

<sup>4</sup> Beijing Astronomical Observatory, Zhong-Guan-Cun, Beijing 100080, China

Received 9 May 1996 / Accepted 22 July 1996

**Abstract.** During the multi-site MUSICOS 92 campaign, the pre-main sequence Herbig Ae star AB Aur was monitored primarily in the He I 5876 Å line, but two of the telescopes were equipped with cross-dispersed echelle spectrographs. The wide spectral domain covered by these instruments allows us to study simultaneously the variability of many photospheric lines.

These data are supplemented with additional observations obtained at Observatoire de Haute-Provence 2 years later.

We find that the photospheric lines of AB Aur have variable profiles, and that distortions cross the line profiles from blue to red, on a time scale of a few hours. These distortions tend to extend significantly blueward of the projected rotation velocity boundary of the line. This implies that localized outflows with velocities of the order of 100 km s<sup>-1</sup> must be present in the photosphere and affect photospheric line formation.

The photosphere of AB Aur may be affected by azimuthal structures creating the observed variability through the effect of stellar rotation, as are the overlying chromosphere and wind, although more data are needed to establish this point unambiguously.

**Key words:** line: profiles – stars: chromospheres – stars: magnetic fields – stars: pre-main sequence – stars: AB Aur – stars: emission line

---

## 1. Introduction

The Herbig Ae/Be stars are pre-main sequence objects with masses ranging from 2 to 5 M<sub>⊙</sub>. A very significant fraction

*Send offprint requests to:* C. Catala

<sup>\*</sup> Based on observations obtained during the MUSICOS 92 MULTI-Site COntinuous Spectroscopic campaign from the University of Hawaii 2.2m and the William Herschel 4.2m telescopes, and from the 1.93m telescope at Observatoire de Haute-Provence

of them show conspicuous signs of strong stellar winds, like P Cygni profiles at H $\alpha$  and Mg II h & k, and of chromospheric activity, like, e.g. the presence of C IV and Si IV resonance lines, emission in Ca II K & infrared triplet, and in He I 5876 Å lines (Catala et al. 1986a).

AB Aurigae is the brightest Herbig Ae star of the northern hemisphere, and is often considered as the prototype of the whole class. A detailed analysis of its line profiles and continua led to a model of its outer layers, including a wind with a mass loss rate of 10<sup>-8</sup> M<sub>⊙</sub> yr<sup>-1</sup>, and an extended chromosphere with a maximum temperature of 17,000 K overlying a photosphere at 10,000 K (Catala & Kunasz 1987). Radiative losses in this extended and expanding chromosphere were estimated to several percent of the star's bolometric luminosity (Catala 1989).

The origin of this tremendous energy flux raises a serious problem, and the recent years have seen a debate about whether it could be dissipated gravitational energy from an accretion disk (Hamann & Persson 1992), or extracted from the stellar internal rotational energy by shear instabilities (Vigneron et al 1990; Lignières et al. 1996). A piece to this puzzle was brought by Böhm & Catala (1993, 1994), who showed on one hand that photospheric lines in AB Aur are not compatible with the presence of a circumstellar disk with the accretion rate needed to provide this high energy input, and on the other hand that the profiles of O I forbidden lines of many Herbig Ae/Be stars exclude the existence of optically thick accretion disks around these stars.

If the origin of the activity is inside the star, we may wonder if a magnetic field plays a role in transporting the energy to the surface and dissipating it in the atmosphere, as in the solar case. As a matter of fact, clues for the existence of such a magnetic field exist for AB Aur and some other Herbig Ae/Be stars: the rotational modulation of lines formed in the wind (Mg II resonance lines, Ca II K) was tentatively interpreted as due to co-rotating streams, organized in a structure controlled by a surface magnetic field, by analogy to the structure of the solar wind (Praderie et al. 1986; Catala et al. 1986b; Catala et al. 1989; Catala et al.

1991). On the other hand, Catala et al. (1993b) searched for the circular polarization signature of a surface magnetic field in AB Aur, but obtained only upper limits of the order of 1kG for such a field. Besides, the link between the stellar wind modulation and phenomena occurring at the stellar surface has not been established, and the observation of short-term variability of lines formed at or close to the photosphere was highly needed to sort out this problem.

The MUSICOS 92 campaign on AB Aur constituted an important step in this research. MUSICOS (for MUlti-Site COntinuous Spectroscopy) is an international collaboration for multi-site, continuous, high-resolution stellar spectroscopy (Catala et al. 1993a). The main goal of the AB Aur observations during the MUSICOS 92 campaign was the monitoring of the He I 5876 Å line, which is formed near the base of the chromosphere (Catala et al. 1993b). A preliminary analysis of these observations is given in Catala et al. (1994), and the full set of data is presented and analyzed in Böhm et al. (1996). The He I 5876 Å line was found spectacularly variable, and these variations provide an important clue that the He I 5876 Å line is rotationally modulated. Other “active” lines formed at various levels in the atmosphere of AB Aur, such as H $\beta$ , Fe II 5018 Å, He I 6678 Å, O I 7773 Å, and Ca II IR triplet, were also found variable and their variations seem closely related to those of the He I 5876 Å line, suggesting that the atmosphere is indeed affected by a fixed azimuthal structure which is co-rotating with the star. These results confirm the idea that the rotational modulation of the wind is probably linked to phenomena occurring at the stellar surface.

The present paper deals with the short-term variability of photospheric lines that were observed on two telescopes involved in the MUSICOS 92 campaign, equipped with echelle cross-dispersed spectrographs, and re-observed 2 years later from Observatoire de Haute-Provence (OHP). The goal of the analysis of photospheric lines is to probe directly the stellar photosphere, and investigate whether this layer is also structured azimuthally, as are the overlying chromosphere and wind.

In Sect. 2, we present the observations and data reduction. The observed variability is described in Sect. 3, and discussed in Sect. 4 in terms of localized outflows affecting the formation of photospheric lines. A general conclusion is given in Sect. 5.

## 2. Observations and data reduction

The MUSICOS 92 campaign took place in December 1992, and involved seven major telescopes (see Böhm et al., 1996, for a complete description of this campaign). Among these, two were equipped with echelle cross-dispersed spectrographs, and therefore covered a wide spectral domain. In addition to the He I 5876 Å line, these instruments were able to provide a monitoring of numerous photospheric lines during the part of the campaign devoted to AB Aur. Table 1 below indicates the characteristics of these two instruments.

The MUSICOS spectrograph, described in Baudrand & Böhm (1992), was transported to Hawaii especially for the campaign. Usually coupled to a 1024<sup>2</sup> CCD detector, this spectro-

graph provides a coverage of the whole visible domain in 2 exposures, one blue (3800 to 5400 Å) and one red (5400 to 8800 Å). However, the use of the UH 2048<sup>2</sup> CCD for the campaign allowed us to cover most of this domain in a single exposure in its red setup (see Table 1).

In this unusual configuration, we noted the presence in the flat-field exposures of a truncated weak additional spectrum, with orders having the opposite curvature with respect to those of the main spectrum. This polluting spectrum, which we attribute to a reflection within the spectrograph, affects about 10 orders in the blue part of the flat-field spectra, by superimposing on them several parallel lines of light. This effect is not seen in the stellar spectra nor in the Th/Ar exposures. It had never been experienced in previous runs with this spectrograph in its normal configuration. The unfortunate consequence is to make the flat-field spectra useless for a good fraction of the blue spectrum.

At the William Herschel Telescope, the Utrecht Echelle Spectrograph was used with its 31.6 grooves mm<sup>-1</sup> grating. The detector was binned by two pixels in the direction perpendicular to the grating dispersion. A neutral density filter was used during flat-field exposure. This filter causes a fringe pattern in the flat-field spectra, which is not present in the stellar spectra. This unfortunate effect prevented us from using the flat-field exposures to correct for pixel-to-pixel CCD variations.

Only two nights out of the three devoted to AB Aur at UH 2.2m were clear. At WHT, only one night was attributed to this program. Table 2 shows the log of these observations for the photospheric lines.

At OHP in November 1994, we used the 193cm telescope, equipped with the Elodie echelle spectrograph (Baranne et al. 1995). This cross-dispersed spectrograph is fed from the Cassegrain focus with an optical fiber. It is used in conjunction with a 1024<sup>2</sup> Tektro CCD, and its 67 orders cover the wavelength range from 3850 to 6800 Å continuously, with a resolving power of about 45,000. During this run, only one night was clear, and the corresponding log of the observations is given in Table 3. Additional observations were planned simultaneously at the Xinglong (China) 2.16m telescope, with the Coudé echelle spectrograph, but bad weather conditions prevented us from obtaining useful data.

A dedicated reduction software, developed by one of us (JFD), was used for the data collected during the MUSICOS 92 campaign. The signal along the orders of the spectrograms was extracted using the optimal extraction algorithm (Horne 1986, Marsh 1989). The Th/Ar spectra were extracted by collapsing the data along the location of the orders. The wavelength calibration procedure consists basically in a 2D polynomial fit of Thorium and Argon lines identified in the spectrum (i.e. both in the direction of the grating dispersion and in the direction of the prism cross-dispersion). The same procedure was applied to both the stellar spectra and the flat-field spectra, but we did not divide the stellar images by flat-field images, in order not to contaminate stellar data by flat-fields affected by the problems mentioned above. The wavelength scales of the stellar spectra were subsequently transformed to a frame linked to the interstel-

**Table 1.** Instrument characteristics

site	telescope	spectro.	detector	resolving power	number of orders	wavelength coverage
Mauna Kea	2.2m UH	MUSICOS	2048 <sup>2</sup> Tektro	32,000	65	4378 to 8894 Å
La Palma	4.2m WHT	UES	EEV 1280 × 1180	40,000	50	4761 to 8172 Å

**Table 2.** Log of the observations: MUSICOS 92

UH 2.2m 6 Dec. 92		UH 2.2m 7 Dec. 92		WHT 4.2m 7-8 Dec. 92	
UT mid-exp	texp (min)	UT mid-exp	texp (min)	UT mid-exp	texp (min)
06:19	30	06:52	30	23:29	10
07:10	60	07:28	30	23:40	10
07:59	30	08:03	30	23:56	10
08:34	30	08:38	30	00:09	10
09:20	30	09:11	30	00:23	10
09:55	30	09:45	30	00:38	10
10:35	30	10:21	30	00:49	10
11:03	15	10:54	30	01:02	10
11:23	20	11:30	30	01:19	10
11:58	20	12:11	45	01:31	10
12:22	20	13:00	45	01:43	10
12:47	20	13:53	45	01:55	10
13:11	20			02:07	10
13:34	20			02:19	10
14:07	20			02:31	10
14:30	20			03:34	10
				03:45	10
				04:02	10
				04:14	10
				04:27	10
				04:41	10
				04:53	10
				05:10	10
				05:21	10

lar Na I D lines, which are assumed to have a constant velocity in the star's rest frame.

At this point of the reduction, the spectra are uncorrected for the blaze function of the orders, and uncorrected for pixel-to-pixel CCD variations. In a second step of the reduction, we divided each spectrum of any given night by the first spectrum obtained that night. This procedure is particularly effective in the case of a fiber-fed spectrograph such as MUSICOS, but proved also to work satisfactorily for the UES data. The resulting residuals are corrected from the blaze response, from pixel-to-pixel variations, and represent the spectral variations during the night.

For the OHP data in November 1994, we used the on-line reduction package provided with the Elodie spectrograph (Baranne et al., 1995). The stellar spectra and the flat-field spectra are extracted using the optimal extraction algorithm.

**Table 3.** Log of the observations: OHP 94

OHP 193cm 10-11 Nov. 94	
UT mid-exp	texp (min)
22:24	60
23:13	30
23:45	30
01:07	30
01:39	30
02:12	30
02:45	30
03:18	30
04:09	60

A Thorium-Argon lamp spectrum is used for wavelength calibration. The wavelength scale was subsequently transformed to the frame defined by the interstellar Na I D lines.

We then identified all the photospheric lines present in the spectra. In order to do so, a mean spectrum was built for each night, and its orders were divided by a smoothed and normalized version of the flat-field orders in order to correct them from the blaze response. Each line was identified, and fitted by a gaussian, whose depth, width and centroid were stored. The depth of this gaussian represents the line depth expressed in ADU, so that it is proportional to both the actual line depth and the square of the signal-to-noise ratio. We discarded the lines presenting strong asymmetries or abnormal widths, these peculiarities indicating the presence of strong blends.

Going back to the residual spectra, we constructed a mean signal by averaging all the lines present in each spectrum, each line being weighted by its depth measured as explained above, and after transforming the wavelength scale into a velocity scale. This procedure gives us a series of average residuals for each night of observation. Table 4 gives a list of the lines that were used for this averaging procedure.

The Si II  $\lambda$  6371.37 Å line is a strong line free of blend in the spectrum of AB Aur (Böhm & Catala 1993). We therefore used the night-averages of this line to set up the wavelength scale in the rest frame of the star. We found that this frame is blueshifted by  $10 \pm 2$  kms<sup>-1</sup> with respect to that of the interstellar Na I D lines, in all three data sets (UH, WHT, OHP). The spectra of the average line residuals were subsequently corrected for this shift.

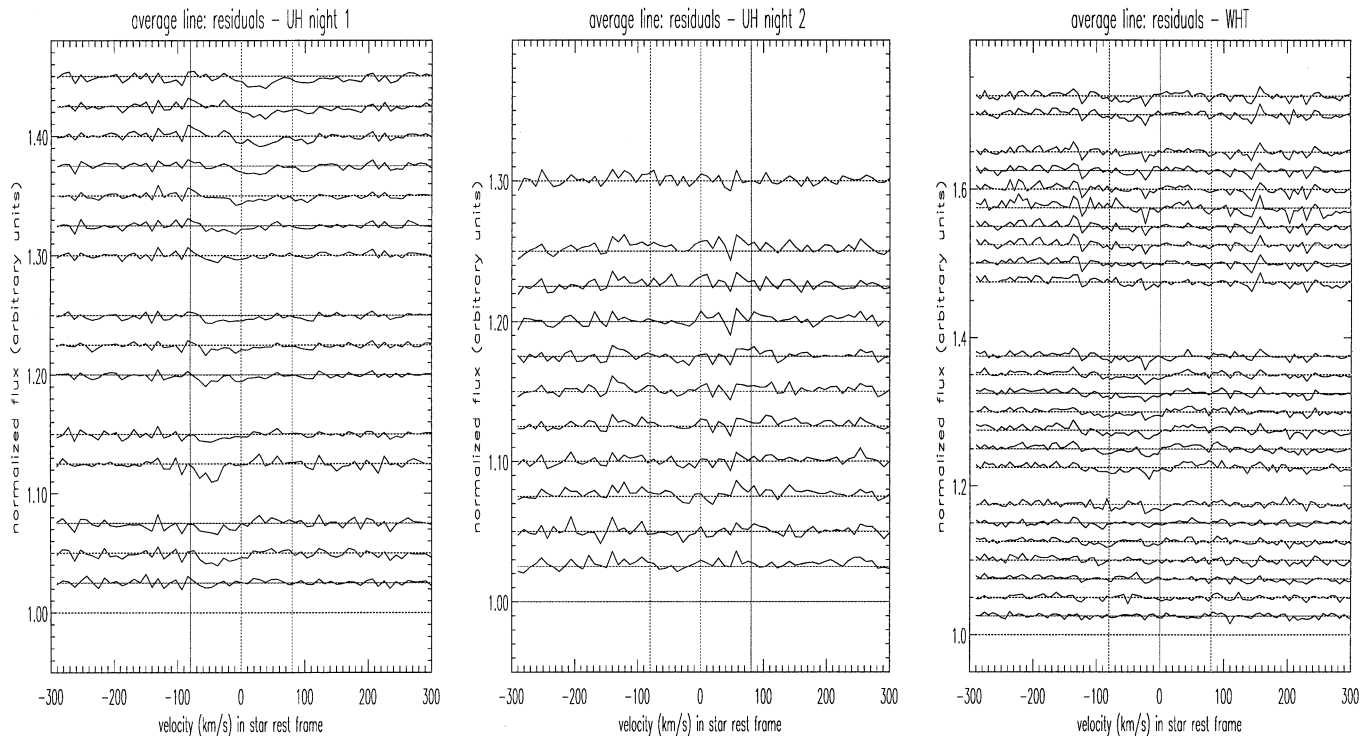


**Fig. 1.** The average line residual spectra from the MUSICOS 92 data. The vertical dashed lines represent zero velocity and the  $\pm v_{\text{ sini}}$  boundaries of the line. The vertical scale corresponds to the relative variations of the spectra. The steps between the spectra are not proportional to the actual time differences between the spectra. The total duration of the UH night 1 coverage is 8.2 hrs, that of UH night 2 is 7 hrs, and that of WHT is 5.9 hrs.

**Table 4.** Photospheric lines used in this analysis

ion	$\lambda(\text{\AA})$	ion	$\lambda(\text{\AA})$	ion	$\lambda(\text{\AA})$
Fe I	4045.81	Ti II	4443.7	Si II	5041.02
Fe I	4071.74	Mg II	4481.13	Mg I	5183.60
Fe I	4143.87	Ti II	4501.27	Fe I	5227.19
Ti II	4163.65	Fe II	4508.29	Fe II	5234.62
Fe II	4178.86	Ti II	4533.97	Fe II	5276.00
Fe II	4233.17	Fe II	4549.47	Fe II	5780.13
Fe I	4404.75	Ti II	4571.97	O I	6158.17
Fe II	4416.83	Cr II	4618.80	Si II	6347.11
		Fe II	4629.34	Si II	6371.37
		Fe I	4957.60		
OHP		OHP,UH		OHP,UH,WHT	

### 3. Variability of the photospheric lines

Fig. 1 displays the residual average line for each of the three MUSICOS 92 nights analyzed here. The vertical lines correspond to the rest wavelength of the line in the star's frame and to the  $\pm v_{\text{ sini}}$  boundaries of the line ( $80 \text{ km s}^{-1}$ , see Böhm & Catala 1993). The photospheric line variability is particularly obvious on the first UH night, where a distortion crosses the line from blue to red, while remaining within the  $\pm v_{\text{ sini}}$  boundaries of the line. On the second UH night 24 hour later, no such variability is apparent. Variations are also seen on the WHT data, obtained

the following day, and are extending significantly blueward of the line near the beginning of the night, then evolving toward the red until the end of the night. The maximum amplitude of the distortion observed in these series of spectra is of the order of 1%.

Profile changes from one spectrum to the next are visible in particular on the second half of the first UH night, during which the exposure time was of 20 minutes. The time scale for the variations is therefore of this order of magnitude.

On the other hand, the variations seem to be monotonic in the course of the night. If they are periodic, which cannot be shown with the data analyzed here, then the period must be significantly longer than 10 hours.

The results obtained from the OHP data of November 94 are displayed in Fig. 2. Variations of amplitudes up to 3% are clearly apparent on these data. Here again, they are monotonic in the course of the night (6 hours), and we see significant changes from one spectrum to the next, typically separated by 30 minutes. The conclusions derived from the MUSICOS 92 data are therefore re-inforced by these additional observations. However, in contrast with the data of Dec. 92, the variations here seem to affect the whole line always in the same manner, with a variable amplitude. We see no blueward or redward displacement of the perturbation, but rather the observed variations consist at first order of a peak on the red side of the line and a depression on its blue side, variable in intensity. This effect can be

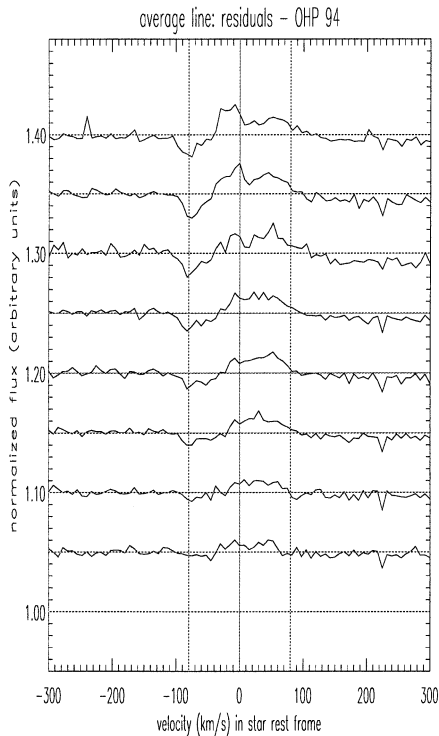


**Fig. 2.** The average line residual spectra from the OHP Nov. 94 data. The vertical dashed lines and the vertical scale have the same meaning as in Fig. 1. Here the total duration of the monitoring is 5.8 hrs.

expected for instance if the line suffers a global Doppler shift, with no significant profile variation. We simulated this effect for a line with a depth of 0.2, corresponding to the strongest lines included in the analysis, and found that a  $15 \text{ km s}^{-1}$  global shift will lead to a variation showing the same characteristics as those observed in the OHP Nov. 94 series, with an amplitude of 3%, similar to the observed amplitude. Such a global Doppler shift cannot be due to a variation of the radial velocity of the interstellar Na I D lines, which are used as a velocity reference in this work, because the measured maximum velocity variation of this line with respect to its laboratory wavelength is smaller than  $1 \text{ km s}^{-1}$  during the course of these observations. Note, however, that the line profile perturbation in this series is not absolutely symmetrical, as it should be if it was due solely to a global Doppler shift of the line. For instance, the last two spectra of the series show a clear asymmetry. This additional pattern indicates that the cause of the variations is more complex than a simple Doppler shift.

In order to ascertain the reality of the variations seen in Figs. 1 and 2, we calculated for each data set the root-mean-square variations in the time series of residual spectra of the average line, i.e. after division by the first spectrum of each data set. Each time series corresponds to the residual intensity in a bin of  $10 \text{ km s}^{-1}$  in velocity space. Such an analysis results in a loss of the time information for the variations, but allows us to quantify the amount of variation within the line, compared to the root-mean-square calculated in the adjacent continuum, which can be

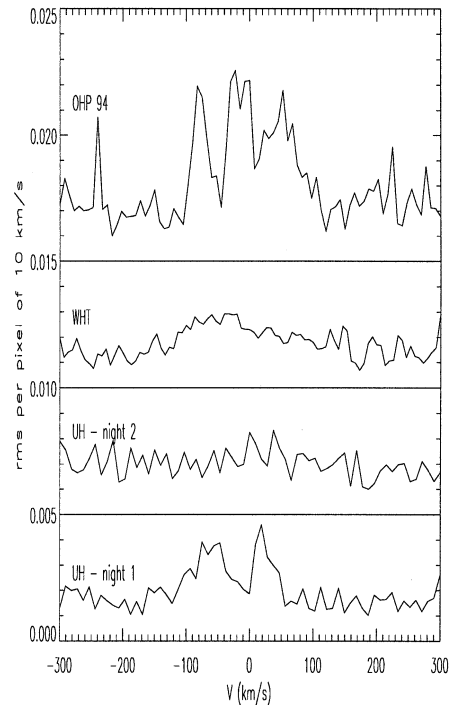


**Fig. 3.** The rms variations of the average line residual spectra, for the four data sets. The vertical scale has been shifted by steps of 0.005 from each data set to the next.

taken as representative of the noise. The results of this analysis are shown in Fig. 3, where the 4 rms curves are plotted together. It can be checked that the rms variations in the line are about 3 times those in the continuum ( $1.5 \times 10^{-3}$ ) during the first night at UH, of the order of twice those in the continuum ( $1.5 \times 10^{-3}$ ) at WHT, and 3.5 times those in the continuum ( $2 \times 10^{-3}$ ) at OHP in 1994. We therefore conclude that the variations of the average photospheric line of AB Aur are real. On the other hand, there is no obvious signal in the second night at UH, with a level of  $2 \times 10^{-3}$  rms.

#### 4. Discussion

It has been shown by Böhm & Catala (1993) that the photospheric spectrum of AB Aur is very well represented by a classical photospheric model (Kurucz, 1979) with  $T_{\text{eff}}=10,220 \text{ K}$  and  $\log g=4.1$ . This indicates that the photospheric lines are effectively formed in the photosphere, with negligible contribution from the overlying layers.

The reported variations of these lines are therefore related to phenomena occurring within the photospheric layers of AB Aur. From the observed characteristics of the line profile variations, we infer that the variable phenomena occur on time scales as short as 20 minutes, and are monotonic on a time scale of at least 8 to 10 hours. Several causes can be invoked to explain such photospheric variations.

The first possible cause is rotational modulation. Although the data presented here are not sufficient to prove that the ob-

served variations are periodic, their time scale and monotonic appearance in the course of each night is compatible with rotational modulation, the rotation period of AB Aur being estimated to 32 hrs (Catala et al. 1986b; Böhm et al. 1996).

Rotational modulation of photospheric lines is expected if localized structures are present in the photosphere. These structures may result from localized abundance anomalies, such as those observed in many Ap stars, or else from temperature, density, or velocity structures in the photosphere.

We note however that the lines that were averaged are produced by 6 different elements: Fe, Ti, Si, Mg, O, Cr, the major contributors being Mg, Fe, and Si. We checked that the variations are not due to only one of these elements, with the lines of the other elements remaining constant, by verifying that they can be seen, although with a degraded S/N ratio, when any single one of these elements is isolated. Besides, the variations observed with lines from single elements have the same characteristics as those of the overall average. We conclude that the variations do not correspond to abundance inhomogeneities, which would on the contrary lead to different variation patterns for different elements. The photospheric structures leading to the observed variations are therefore likely to correspond to temperature, density or velocity inhomogeneities.

Fig. 4 is a grey-scale representation of the photospheric variations observed in the MUSICOS 92 data, calculated as described in Sect. 2, as a function of rotational phase. We have assumed a rotation period of 32 hrs (Catala et al., 1986b), and the phase origin has been set to the first spectrum of the first UH night. Vertical full lines indicate zero velocity and the  $\pm v_{\text{ sini}}$  boundaries of the photospheric lines. The first UH night corresponds to the phase interval [0,0.3], the WHT night to phases 0.3 to 0.5, and the second UH night to phases 0.8 to 1. This representation must be read with caution, because each spectrum was divided by the first spectrum of the same night. Therefore, any feature existing on the first spectrum of a series will show up in the whole series of residuals. Also, we cannot expect any continuity between adjacent phases originating from 2 different series.

The variation pattern can be seen very clearly in Fig. 4. From phases 0 to 0.3 (UH night 1), we see an absorption feature travelling from the blue side to the red side of the line, remaining within the  $\pm v_{\text{ sini}}$  boundaries of the line. We note on the last spectrum of this series the presence of an additional absorption feature at about  $-100 \text{ km s}^{-1}$ , which reappears at the beginning of the WHT data. This blue feature then travels toward the red from phase 0.3 to phase 0.5. On the same data, a standing feature is also present near zero velocity. Finally, a weak "emission" feature also appears from phase 0.3 to 0.5 on the red side of the line.

Besides, the variations extending blueward of the blue  $-v_{\text{ sini}}$  boundary of the line, significant outward velocity fields must be present in these photospheric structures. On the WHT data, we see features at about  $-100 \text{ km s}^{-1}$ , while a  $v_{\text{ sini}}$  of  $80 \pm 5 \text{ km s}^{-1}$  was determined by Böhm & Catala (1993). Because radial outflows do not contribute to the blueshift when they occur at the limb where the projected rotation velocity is maximum, but

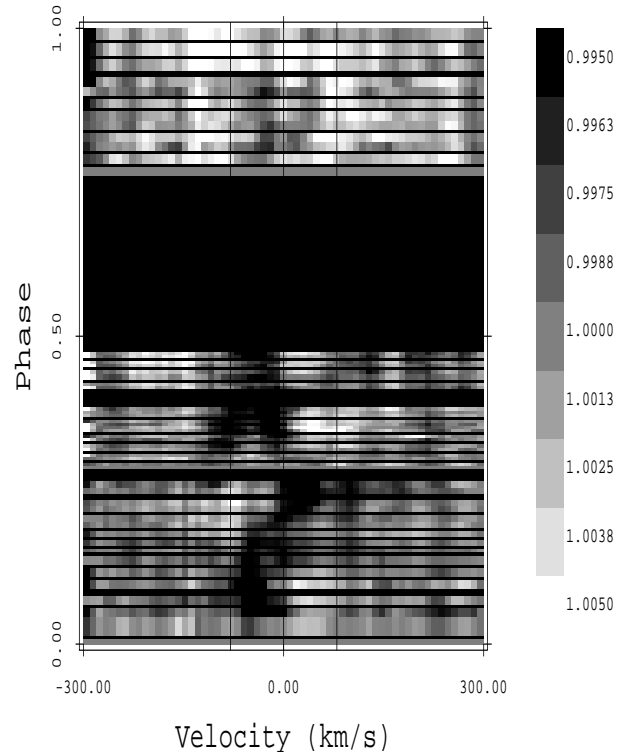


**Fig. 4.** The average residual spectra as a function of rotational phase, assuming a rotation period of 32 hr.

have their maximum contribution when they face the observer, we conclude that the velocity fields responsible for this blue extension of the variations must be of the order of  $-100 \text{ km s}^{-1}$ .

It is very tempting to investigate whether these photospheric structures could be the foot points of the structures responsible for the modulation of chromospheric and wind lines. If this was the case, we would see a correlation between the variation of photospheric lines and lines formed in the chromosphere and the wind of AB Aur. We have compared our results on photospheric lines with the variations of the He I D3 line observed extensively during the campaign and described in detail in Böhm et al. (1996). The He I data obtained simultaneously with the photospheric data analyzed in this paper are presented in Fig. 5, as a function of rotational phase. The He I data were treated in the same way as the photospheric lines, i.e. each spectrum was divided by a reference spectrum obtained at one of the three reference phases used in the photospheric line analysis (each reference phase corresponding to the first spectrum of each UH or WHT series). The He I variations during the first UH night seem to follow those of the photospheric lines, in the sense that an absorption component in the residual spectra appears and moves toward the red. On the other hand, variations of the He I line in the second UH night are very clearly seen, while there seems to be no detectable variation of photospheric lines. The He I data recorded at WHT present some weak variations, especially near the end of this night, which do not seem related to the weak photospheric variations detected for the same time

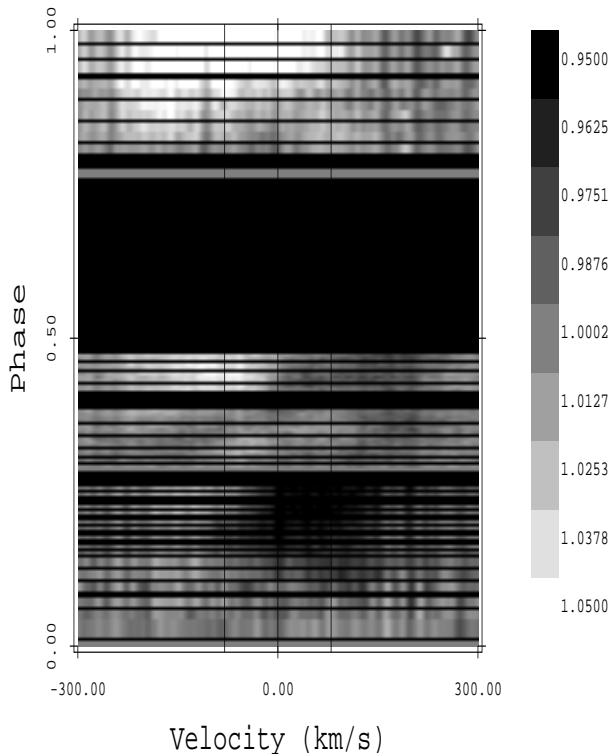


**Fig. 5.** The He I line profiles presented on the same phase scale as the photospheric data. Only the data obtained in the same time interval as the photospheric data are presented here

interval. We therefore have no clear evidence for a correlation between the two sets of data. However, we have no photospheric data at the phase showing the huge absorption component in the He I profile (not shown in Fig. 5), which is the most important feature in this series of data (Böhm et al., 1996). The lack of data weakens significantly our conclusion.

Fig. 6 presents the variations of the He I D3 line in the OHP series of November 1994. Here, a clear similarity can be seen with the variations of the photospheric lines shown in Fig. 2. In particular, the increase in the emission on the red side of the line is seen in both sets of data.

Taking all these results together, we seem to have some indication that the same structure could be at the origin of the modulation at photospheric and chromospheric levels, but clearly more data are required to conclude firmly on this point.

Nonradial pulsations (NRPs) constitute another possible cause of photospheric line variability. Because the variations appear monotonic in the course of 8 hours, the period of the pulsations must be longer than 16 hours. Only g-modes, in which the restoring force is gravity, can have such long periods. This would not be the first time such long period NRPs are reported for stars in that part of the HR diagram. A group of A- and F-type dwarfs have been recently found to be variable with periods of the order of one day, and for at least one of them,  $\gamma$  Dor, there is conclusive evidence that the variations are indeed due to g-modes (Balona et al. 1996).

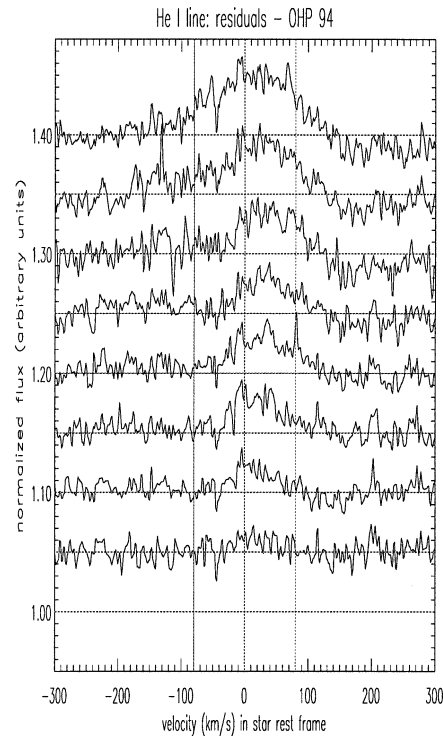


**Fig. 6.** The He I line residual spectra from the OHP Nov. 94 data

We also note that photospheric line variations were reported for another Herbig Ae star, HD 163296, and tentatively interpreted as due to NRPs by Baade & Stahl (1989), although not conclusively due to lack of data. Another Herbig Ae star, HD 104237, also shows some evidence for NRPs (Donati & Catala, in preparation).

In the case of AB Aur reported here, the variability outside the  $\pm v_{\text{ini}}$  of the lines adds some complexity to the picture. Similar characteristics were also reported for HD 163296 by Baade & Stahl (1989). In both cases, this variability at high velocity may be the sign that the photospheric pulsation affects the overlying layers, and forces wind variability with the period of the pulsation.

Another difficulty with the NRP interpretation is the absence of photospheric variation in the second night at UH, only 24 hours after the variable episod of the UH first night. Note however that the noise in our data is higher in the second UH night, so that variations at a somewhat lower level than observed on the first night can be present without being seen.

Our observations are therefore rather difficult to reconcile with the NRP interpretation, but this hypothesis cannot be completely rejected on the basis of the present data.

Finally, we cannot rule out either the possibility that the observed variations are not periodic, but simply due to transient phenomena, for instance taking place in the wind and having some feedback at photospheric level.

Among all these possible interpretations of the observed photospheric variability, the most likely is certainly rotational modulation, based on the fact that rotational modulation of lines

formed in the wind of AB Aur has been detected earlier (Catala et al. 1986b). However, due to the incompleteness of our data, we have been unable to show that the photospheric line variations are periodic and correlated to the variations of lines formed higher in the star's atmosphere. A more definite conclusion will have to wait for more data.

## 5. Conclusion

We have shown in this paper that the photospheric lines of AB Aur are variable. We have failed to show that the observed variations are periodic, but they occur on a time scale compatible with the star's rotation. These variations may be due to the presence of photospheric active regions involving outflows with velocities of the order of  $100 \text{ km s}^{-1}$ , although other possible interpretations, like nonradial pulsations or transient phenomena occurring in the stellar wind cannot be ruled out on the basis of the material presented here.

This new result brings yet another indication that the atmosphere of this star is probably structured by a surface magnetic field. If this is true, then two major questions need to be answered in the future:

- What is the origin of this magnetic field? The original stellar evolution calculations of Iben (1965) or the more recent ones by Gilliland (1986) predict that a  $2.5 M_{\odot}$  star like AB Aur does not possess any outer convection zone. Later, Palla & Stahler (1991, 1993) claimed that deuterium burning could produce such a convection zone, but the timescale for deuterium burning is too short for giving rise to a significant active episode. The origin of the hypothetical magnetic field is thus paradoxical. A possible scenario would involve a non-solar dynamo, in which shear-instabilities at the interface between a turbulent sub-photospheric region powered by the braking torque of the wind and an unperturbed interior would play a major rôle (Vigneron et al. 1990, Lignières et al. 1996).
- What is the physical reason for line profile variations? It is difficult to invoke temperature inhomogeneities in the absence of subphotospheric convective layers: solar-type spots indeed are due to a magnetic blocking of convective energy transport; in the case of non-convective turbulent subphotospheric envelope, the fraction of the energy transported by the turbulent eddies, and susceptible of being blocked by a magnetic field, is negligible (Lignières et al. 1996). We have shown in this paper that these variations are not due to abundance inhomogeneities. The effect of the stellar wind, and the presence of photospheric macroscopic outflows that might affect significantly the energy balance, may be the answer to this question, but some major investigation should be carried out in the future to study this problem.

*Acknowledgements.* We thank the staffs of the University of Hawaii 2.2m, the William Herschel 4.2m, and the OHP 1.93m telescopes for their efficient assistance during the observations. We are grateful to all the participants to the MUSICOS 92 campaign for their involvement in the project. We acknowledge financial support from the “Institut des

Sciences de l'Univers” (INSU/CNRS), the CNRS “Groupements de Recherche” “Magnétisme dans les étoiles de type solaire”, “Structure interne des étoiles et des planètes géantes”, and “Milieux circumstellaires”, the Paris Observatory, and the University of Hawaii.

## References

- Baade, D., Stahl, O. 1989, *A&A* 209, 268
- Balona, L.A., Böhm, T., Foing, B.H., Ghosh, K.K., Janot-Pacheco, E., Krisciunas, K., Lagrange, A.M., Lawson, W.A., James, S.D., Baudrand, J., Catala, C., Dreux, M., Felenbok, P., Hearnshaw, J.B. 1996, *MNRAS*, in press
- Baranne, A., Queloz, D., Mayor, M., Adriansyk, G., Knispel, G. 1995 submitted to *A&AS*
- Baudrand, J., Böhm, T. 1992 *A&A*, 259, 711
- Böhm, T., Catala, C. 1993 *A&AS*, 101, 629
- Böhm, T., Catala, C. 1994 *A&A*, 290, 167
- Böhm, T., Catala, C., Carter, B., Baudrand, J., Butler, J., Collier-Cameron, A., Czarny, J., Donati, J.-F., Foing, B.H., Ghosh, K.K., Houdebine, E., Huang, L., Jiang, S., Hao, J., Neff, J., Rees, D., Semel, M., Simon, T., Talavera, A., Welty, A., Zhai, D., Zhao, F. 1996, *A&AS*, in press
- Catala, C., Czarny, J., Felenbok, P., Praderie, F. 1986a, *A&A* 154, 103
- Catala, C., Felenbok, P., Czarny, J., Talavera, A., Boesgaard, A.M. 1986b, *ApJ* 308, 791
- Catala, C., Kunasz, P.B. 1987, *A&A* 174, 158
- Catala, C. 1989, in *Modeling the Stellar Environment: How and Why?*, 4<sup>th</sup> IAP meeting, Paris, eds: Ph. Delache, S. Laloe, C. Magnan, J. Tran Thanh Van, p. 207
- Catala, C., Simon, T., Praderie, F., Talavera, A., Thé, P.S., Tjin A Djie, H.R.E. 1989, *A&A* 221, 273
- Catala, C., Czarny, J., Felenbok, P., Talavera, A., Thé, P.S. 1991, *A&A* 244, 166
- Catala C., Foing B.H., Baudrand J., Cao H., Char S., Chatzichristou H., Cuby J.G., Czarny J., Dreux M., Felenbok P., Floquet M., Guérin J., Huang L., Hubert-Delplace A.M., Hubert H., Huovelin J., Jankov S., Jiang S., Li Q., Neff J.E., Petrov P., Savanov I., Shcherbakov A., Simon T., Tuominen I., Zhai D., 1993a, *A&A*, 275, 245
- Catala, C., Böhm, T., Donati, J.-F., Semel, M. 1993b, *A&A*, 278, 187
- Catala, C., Böhm, T., Donati, J.-F., et al. 1994, *Solar Phys.*, 155, 185
- Hamann, F., Persson, S.E., 1992, *ApJS*, 82, 285
- Horne, K. 1986, *PASP* 98, 609
- Kurucz, R.L., 1979, *ApJS*, 40, 1
- Lignières, F., Catala, C., Mangeney, A. C. 1996, *A&A*, in press
- Marsh, T.R. 1989, *PASP* 101, 1032
- Palla, F., Stahler, S. 1991, *ApJ* 375, 288
- Palla, F., Stahler, S. 1993, *ApJ* 418, 414
- Praderie, F., Simon, T., Catala, C., Boesgaard, A.M. 1986, *ApJ* 303, 311
- Vigneron, C., Mangeney, A., Catala, C., Schatzman, E. 1990, *Solar Phys.*, 128, 287